Bioresource Technology 104 (2012) 673–678

Contents lists available at SciVerse ScienceDirect

Bioresource Technology

journal homepage: www.elsevier.com/locate/biortech

A microwave reactor for characterization of pyrolyzed biomass

Xiqiang Zhao, Min Wang, Hongzhen Liu, Longzhi Li, Chunyuan Ma, Zhanlong Song *

National Engineering Laboratory of Coal-Fired Pollution Reduction, Shandong Provincial Key Lab of Energy Carbon Reduction and Resource Utilization, Shandong University, No.17923 Jingshi Road, Jinan 250061, PR China

ARTICLE INFO

Article history:
Received 8 June 2011
Received in revised form 16 September 2011
Accepted 30 September 2011
Available online 13 October 2011

Keywords:
Microwave pyrolysis
Temperature curve
Weight loss
Dynamics
Temperature control

ABSTRACT

A microwave reactor (MWR) was designed to investigate microwave-induced pyrolysis of biomass. Condensation of tars on the quartz reactor and the pipelines was prevented by an electric heating device, and a temperature control function allowed determination of product characteristics at constant temperatures. Temperature had an important influence on microwave pyrolysis; the yields of gas products increased from 17.69 wt.% to 22.27 wt.% and the ratio of combustible gas to total gas products increased from 67.21 vol.% to 77.14 vol.% as the temperature increased from 400 °C to 600 °C. A large number of volatiles was released as temperature increased, resulting in an increase in the number of pores of the coke and a uniform pore structure was obtained. The specific surface area of coke increased from 0.89 m^2/g (400 °C) to 9.81 m^2/g (600 °C) and the pore volume increased from 0.006 cm^3/g (400 °C) to 0.012 cm^3/g (600 °C), but the average pore size decreased from 282.16 nm (400 °C) to 46.64 nm (600 °C).

© 2011 Elsevier Ltd. All rights reserved.

1. Introduction

Pyrolysis is one of the most promising thermo-chemical conversion routes for recovering energy from biomass. It converts biomass to liquid (bio-oil), gaseous, and solid (char) fractions in the absence of oxygen. In the pyrolysis process, primary reactions are concerned with the degradation of biomass into char and numerous volatiles, whereas secondary reactions involve primary volatiles as they move through the high-temperature char layer and/or the reacting environment. Generally, secondary reactions occur inevitably, and more gaseous and solid products are obtained (Di Blasi et al., 2001). Although more liquid (bio-oil) fractions can be obtained through fast pyrolysis, the size of sample should not exceed 1 mm in order to obtain a high heating rate. As a result, the pretreatment of raw materials especially crop straws can be energy-intensive.

The yield and quality of products from pyrolysis can be improved by utilizing catalysts and/or using new heating methods (Encinar et al., 2008; Huang and Tang, 2008; Tu et al., 2009). One such method uses microwaves since this heating method results in a more uniform temperature distribution than conventional thermal conductance from an external heat source. A uniform temperature distribution may prevent undesirable secondary reactions, resulting in the better control of the pyrolysis process and the attainment of desired end products (Yu et al., 2006). More importantly, large-sized biomass, such as bulk wood bulk (Miura et al., 2004) and straw bales (Zhao et al., 2010) can be processed.

Microwave-induced pyrolysis has been employed to pyrolyze wood blocks, and valuable results different from those of conventional heating were obtained (Miura et al., 2004). The catalytic effects of additives such as NaOH, Na_2CO_3, Na_2SiO_3, NaCl, TiO_2, HZSM-5, H_3PO_4, $Fe_2(SO4)_3$ on microwave pyrolysis of pine sawdust (Chen et al., 2008) have been studied. All of the additives have increased the yield of solid products, decreased the yield of gaseous products to some extent, and made these gases evolve earlier. The gases produced by pyrolysis consist mainly of H_2, CH_4, CO and CO_2. Microwave-induced pyrolysis of rice straw has also been studied (Huang et al., 2008, 2010). The major gaseous products were H_2, CO_2, CO, CH_4 at concentrations of 55, 17, 13, 10 vol.%, respectively. Microwave pyrolysis of coffee hulls (Domínguez et al., 2007b), biomass (Wan et al., 2009), waste tea (Yagmur et al., 2008), corn stover (Lei et al., 2009), wheat straw (Budarin et al., 2009) and oil palm biomass (Salema and Ani, 2011) led to gas products with a high H_2 content, implying that microwave-induced pyrolysis of biomass has the potential to produce H_2-rich fuel gas.

Most studies on microwave pyrolysis have focused on the influence of operating parameters on the end products and, with the exception of a study by Wang et al. (2009), studies on microwave-induced pyrolysis at constant temperatures or on process dynamics during microwave pyrolysis have not been done. Knowledge about these dynamics concerning maximum devolatilization rate, initial degradation temperature, temperature of the peak rate, and conversion time, is required for process optimization and design and operation of thermo-chemical conversion units (Di Blasi

---

* Corresponding author. Tel.: +86 531 88399372; fax: +86 531 88395877.
E-mail address: zlsong@sdu.edu.cn (Z. Song).

0960-8524/$ - see front matter © 2011 Elsevier Ltd. All rights reserved.
doi:10.1016/j.biortech.2011.09.137

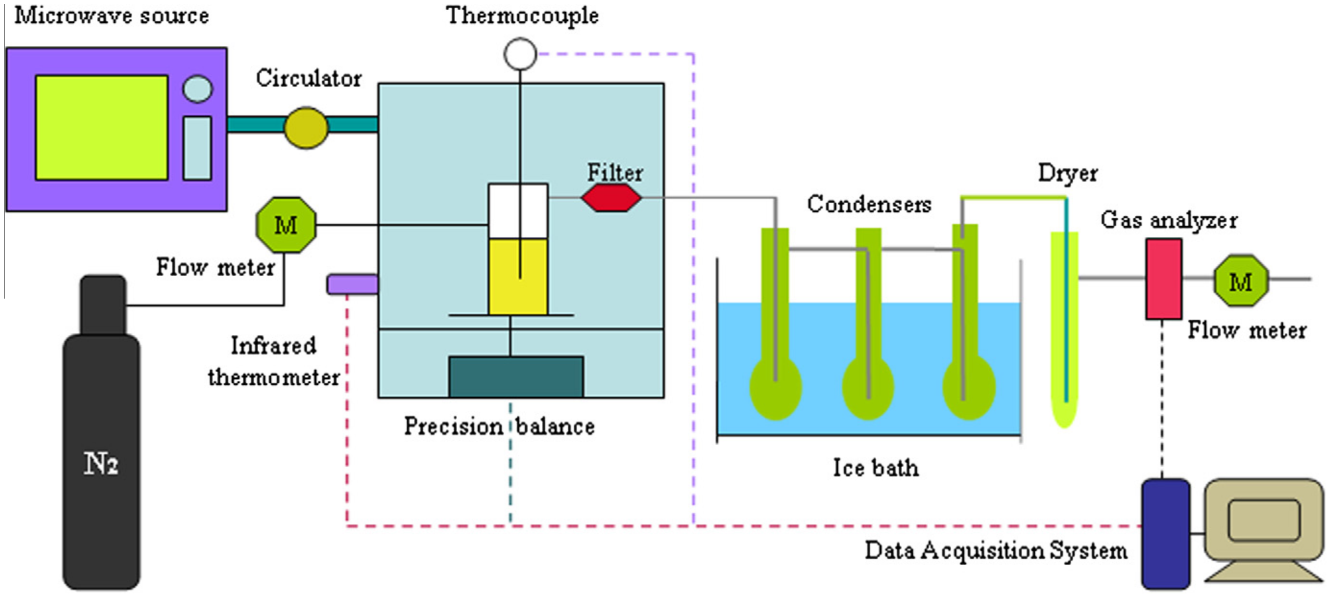

Fig. 1. Schematic diagram of the microwave reactor.

et al., 2001). Investigations of these parameters can be impeded by condensation of tar vapors and adhesion to the reactor walls and pipelines which makes precise measurements of products difficult (Domínguez et al., 2003).

Consequently, the current study was carried out with a MWR with designed to avoid vapor condensation when pyrolyzing wheat straw using microwave heating.

2. Methods

2.1. Materials

Wheat straw, collected from Liangshan County, Shandong Province in Eastern China was air dried under sunlight for 30 days, shredded by spiral breaker, ground by straw stalk grinder, and sieved to 0–200 mesh (0–0.090 mm). The proximate and ultimate analyzes of the wheat straw were conducted, and the chemical structures of wheat straw were also identified by Fourier transform infrared spectrometer (Tensor 27, Bruker, Germany) before the experiments.

2.2. Experimental apparatus

A schematic diagram of the MWR is shown in Fig. 1. The MWR mainly consists of five components: a modified 3000 W, 2.45 GHz domestic microwave oven, a two-figure electronic balance (Shanghai, Yousheng BS1000G, Capacity: 700 g, Precision: 0.01 g), a thermocouple (Type K, 0–1000 °C) for temperature measurement, a electric heating device for circulation air, a product cooling and collection system, and a computer running proprietary acquisition and control software (provided by King View). To prevent the magnetron from being damaged by reflected microwaves, a ferrite circulator (Type: Y) was built between the microwave source and the MWR. Thus, the reflected microwaves are absorbed by the circulating water. The reaction tube (18 cm length, 8 cm outer diameter) and crucible were made of quartz. Both ends of the quartz tube were sealed tightly with a silica o-ring and a polytetrafluoroethylene sealer. A thin thermocouple in a grounded metal sheath and held exactly at 90° to the electric field component of the microwave energy was installed (Menéndez et al., 1999; Liu et al., 2004). The samples, in a quartz crucible, were placed on a salver connected to the balance. The balance and thermocouple were connected to the data acquisition system. The software continuously monitored and recorded the weight and temperature of the samples, and updated the microwave power every second.

2.2.1. Temperature control function

The temperature control function was introduced to carry out microwave pyrolysis of sample at constant temperatures. The system allows setting of a constant microwave power or the power can be adjusted based on a desired temperature value. Thus, when the temperature of the sample reached the target temperature, the microwave power was reduced automatically, and increased again when the temperature dropped. This process operated continuously, allowing operation under a constant, pre-set temperature.

2.2.2. Electric heating device for circulation air

The circulation air was heated by an electric heating device and then introduced into the microwave cavity. Consequently, the experimental apparatus in the microwave cavity was heated. The temperature range of the circulation air was allowed to be adjusted from the room temperature to 400 °C. The device was used to prevent the condensation of liquid-phase products on the walls of the quartz reactor and pipelines and thus facilitated accurate collection of products. Besides, the lifetime of experimental apparatus could be extended as the corrosion of tars to the metal and silicone tubes was avoided.

2.3. Procedure of microwave pyrolysis

For each trial, 5–30 g (precision to 1 mg) of shredded and sieved wheat straw was placed in a quartz crucible. After the quartz crucible was correctly positioned and the quartz tube was tightly sealed, a constant flow (3 L/min) of carrier gas (N_2) was purged into the reactor. When the purging was sufficient to produce an anoxic state, the microwave generator was turned on and switched to the designated power.

As the reaction proceeded, the reaction temperature was recorded at periodic intervals. When the temperature achieved the target value, the temperature control function commenced, and the sample pyrolyzed at a constant temperature. After the designated reaction time passed, the microwave generator was turned off, but the carrier gas kept purging until the solid residue (coke) was self-cooled to below 100 °C. The gas collector was then carefully removed and sealed. The solid residue was placed in a desiccator and weighed after it reached room temperature. To protect the experimental apparatus, the sample was only heated for 10 min after the temperature of the sample reached the set temperature. If experiments under a higher temperature would be carried out, then the temperature control function could simply be canceled. For guarantying the accuracy of experiments, every condition was repeated two times and the result was the average value of these two experiments.

2.4. Analysis of products

The composition of the gas products was analyzed by an Agilent 6890N gas chromatography/dual thermal conductivity detector with a GDX401 capillary column and 5A molecular sieve. The temperature of the injector, oven, and detector was 100, 80, and 150 °C, respectively. The flow rate of the carrier gas was 15 ml/min without splitting.

To determine the main composition of the gas products, online FTIR analysis of the gas products was carried out. The condensed and dried gases were directly introduced into the FTIR analyzer (DX4000, GASMET, Finland). The carrier gas flow was 3 L/min, designed to make gas products as fast as possible at a lower temperature and reduce the occurrence probability of the secondary decomposition of the primary products. The temperature in the test chamber and the gas transmission pipeline was kept at 180 °C to prevent the condensation and absorption of the semi-volatile gas products. The volume flow of gas products was determined with a flow meter at the outlet of the FTIR analyzer. Then the weight of gaseous products was obtained by the total volume multiplied by the average molecular weight and the weight of liquid products was obtained by subtraction of gas products and solid products from the total weight of sample.

The solid products were ground to fine particles using a mortar and subjected to FTIR spectrometer which was used in Section 2.1. The IR spectra were between 4000 and 600 cm^{-1} with a resolution of 4 cm^{-1}. The surface property of coke (i.e., surface area, pore distribution, and volume) was analyzed using an acceleration pore surface area porosimetry instrument (ASAP 2020, Micromeritics, USA), with liquid nitrogen as the adsorbent in the adsorption isotherm under 77 K. Multi-point Brunauer, Emmett, and Teller (BET) surface area analysis method was used. V_T is the total pore volume, and the average pore diameter $d_{ave} = 4V_T/S_{BET}$. The pore properties of coke were also examined using an accelerated scanning electron microscopy (SEM) (JSM-6010LV, JEOL, Japan). The magnification was 500. The main elements of coke were measured by an elemental analyzer (Vario Micro cube EL III, Elementar, Germany).

3. Results and discussion

3.1. Chemical structure of wheat straw

The results of the proximate and ultimate analyzes of wheat straw are listed in Table 1. The volatile content of wheat straw was 69.30 wt.%, supporting the use of wheat straw as an energy source. Wheat straw contains a large number of oxygen-containing functional groups such as OH (3400–3200 cm^{-1}), C–H (2936–2916 cm^{-1} olefin), C=O (1765–1715 cm^{-1}), C–O–C (1270 cm^{-1}), CO–(H) (–1050 cm^{-1}), alkyl, ether, aromatic, ketone, and alcohol (3000–2800 cm^{-1} and 900–700 cm^{-1}), indicating the high-oxygen content of the sample (Supplementary Fig. 1).

Table 1
Proximate and ultimate analyzes of wheat straw.

Proximate analysis (wt.%)				Ultimate analysis (wt.%)				
M_{ad}	A_{ad}	V_{ad}	FC_{ad}	C	H	O^a	N	S
7.4	5.9	69.3	17.4	41.41	5.86	45.22	1.44	0.17

M: moisture content, V: volatile matters, A: ash, FC: fixed carbon; ad: on air dried basis.

[a] Subtraction.

3.2. Temperature profiles during microwave heating

3.2.1. Electric heating device not in operation

The temperature of silicon carbide (SiC) increased rapidly as the microwave radiation was absorbed. As the radiant heat loss increased with increasing temperatures, the temperature profile ceased to be linear above a temperature of 200 °C, and the heating rate decreased until thermal equilibrium was achieved (Fig. 2). The time for achieving thermal equilibrium was shortened with the increase in microwave power. When the microwave power was 900 W, the heating curve was nearly linear, and the heating rate was about 60 °C/min. The inertness of SiC may play an important role as a "microwave absorber" in the microwave heating process of other materials that do not absorb microwaves well (Zuo et al., 2011).

3.2.2. Electric heating device in operation

As shown in Fig. 2, when the electric heating device was operated, the radiant or convection heat loss was small because of the sample's low temperature in the initial period of heating. Thus, the temperature difference of the sample with or without circulation heating device was not obvious. However, after the temperature exceeded a certain value, the temperature curves under the circulation heating operation had a remarkably increasing trend. This trend can be attributed to the heat loss increase through convection and radiation along with the increase in temperature. The temperature difference between the reactor and circulation air declined when the electric heating was turned on, and the heat loss decreased. Consequently, the temperature of the sample obtained through electric heating increased faster than when electric heating was not in operation.

3.3. Temperature curves under temperature control

With SiC as the sample and limit power at 100 W, temperature fluctuations were small and the temperature stabilized at the set target (Fig. 3). Temperature fluctuations are inevitable because of

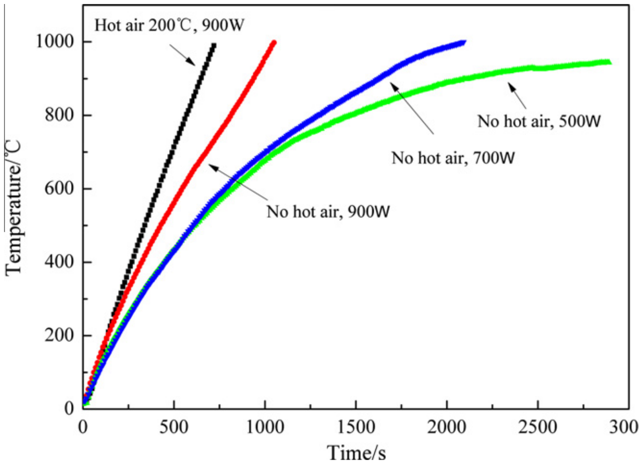

Fig. 2. Temperature curves of SiC under different microwave powers and hot air 200 °C.

thermal inertia of the system. Another possible reason for temperature fluctuation is that SiC strongly absorbed microwaves, so its temperature changed remarkably with the microwave power supply on or off. The combination of the two reasons above caused the amplification of error between the actual temperature and the target temperature. However, the temperature deviation is in an acceptable range and the fluctuation of the temperature may be decreased by adopting a proper microwave limit power obtained through experiments.

3.4. *Pyrolysis characteristics under constant temperatures*

For obtaining precise experimental results at constant temperature, the time of the sample heated from room temperature to the target temperature should be as short as possible to decrease the occurrence probabilities of other reactions such as dehydration and torrefaction. Because pure straw absorb microwave very weak, using pure straw as sample directly will not achieve this requirement. According to previous studies (Yu et al., 2006; Domínguez et al., 2006) and our previous experiment tests, using the following mix of straw (10 g) and pyrolysis residue (5 g) not only allowed a short heating time, but the temperature of the sample was also controlled at the set temperature (Supplementary Fig. 2).

3.4.1. *Products distribution under different pyrolysis temperatures*

The product distribution under different pyrolysis temperatures is shown in Fig. 4. With the increase in pyrolysis temperature from 400 °C to 500 °C, the ratio of solid residue to the total weight of sample deceased from 56.2 wt.% to 46.3 wt.%. With continued increase in pyrolysis temperature, no significant changes in the solid production were found. One possible reason is that the pyrolysis of the sample at the central region intensified with the increase in temperature. However, pyrolysis of the sample close to the surface did not occur because of the intermittent microwave heating after the operation of the temperature control device.

The yield of gaseous products increased slightly with increase in temperature (400–600 °C), but it was not greater than 25 wt.% and was largely different from that when complete pyrolysis occurred (Supplementary Fig. 3). One possible reason is that some volatiles were not released because of the low temperature. Another possible reason is that gasification reactions among H_2O, CO_2 and carbon were infrequent because of the low temperature (Menéndez et al., 2007).

However, when pyrolysis occurred at the temperature of 600 °C for 10 min, the ratio of solid residue to the total weight of sample was still close to 50 wt.%. The possible reason is that the temperature measured by thermocouples was the temperature of sample at the central region. Although the central region of sample reached the temperature of 600 °C, because of the high heat transfer resistance between biomass particles (Encinar et al., 2000) and of "internal heating" by the microwaves, no pyrolysis of the samples close to the surface occurred. However, it can be expected that as the pyrolysis temperature increases, the yield of the gas products will improve significantly, and the production of solids will decrease. Not only the remaining volatiles be released, but the reactions among CO_2, H_2O, and carbon will be promoted by the higher temperature.

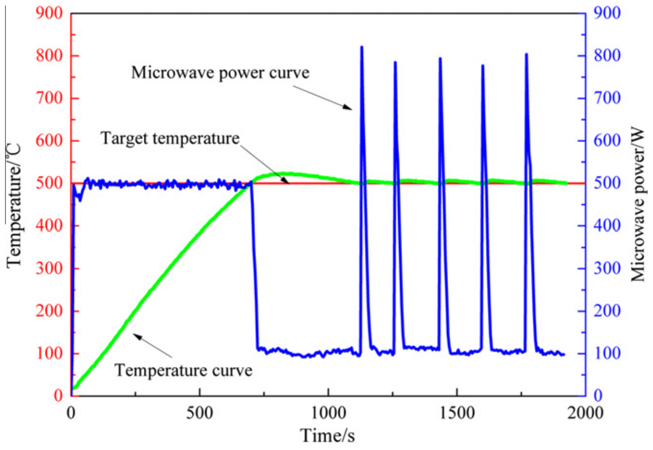

Fig. 3. Curve of SiC at microwave power 100–500 W, the target temperature at 500 °C.

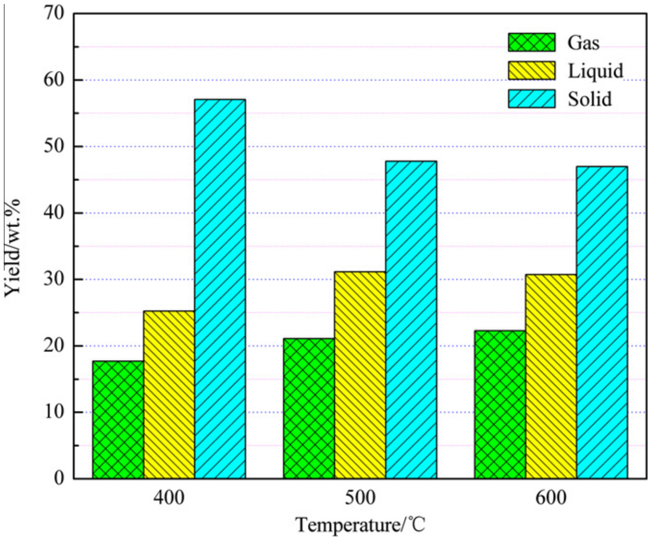

Fig. 4. Product distribution under different pyrolysis temperatures.

3.4.2. *Compositions of the gas products under different pyrolysis temperatures*

The formation of the gaseous products is a consequence of tar cracking, the decomposition of the char at high temperatures and the reactions between the species formed during pyrolysis (Domínguez et al., 2007a). The composition of the gas products at different pyrolysis temperatures is shown in Fig. 5. When the temperature was 400 °C, the main composition of the gas products was CO (34.7 vol.%), CO_2 (33.8 vol.%), H_2 (22.1 vol.%), and CH_4 (7.9 vol.%). With the increase in temperature, the content of H_2 rapidly increased from 22.1 vol.% (400 °C) to 43.7 vol.% (600 °C), and CO_2 content decreased rapidly from 33.8 vol.% (400 °C) to 23.6 vol.% (600 °C). The high concentrations of CO_2 and CO in the pyrolysis gases are mainly due to the high degree of deoxygenation produced during the pyrolysis experiments (decarbonylation and decarboxylation reactions). The strong decrease in CO_2 with temperature in the pyrolysis gases could be related to the carbon gasification reaction. With the further increase in temperature (600–1000 °C), the content of H_2 is expected to improve further, and the amount of CO_2 would decrease (Menéndez et al., 2004).

The content of CO decreased slowly with the increase in temperature, accounting for 25–35 vol.% of the total gas products. The content of CH_4 had a decreasing trend with the increase in temperature, suggesting that high temperature promotes the decomposition and dry reforming reactions of CH_4 (Domínguez et al., 2007a,b).

$$CH_4 + CO_2 \rightarrow 2CO + 2H_2 \quad \Delta H_{298} = 247.9\ \text{kJ mol}^{-1} \tag{1}$$

$$CH_4{-}C + 2H_2 \quad \Delta H_{298} = 75.6\ \text{kJ mol}^{-1} \tag{2}$$

Hydrogen is also produced by the dehydrogenation reactions of char and oil, such as aromatization, condensation, and alkene formation. The characteristics of gas products changing with the

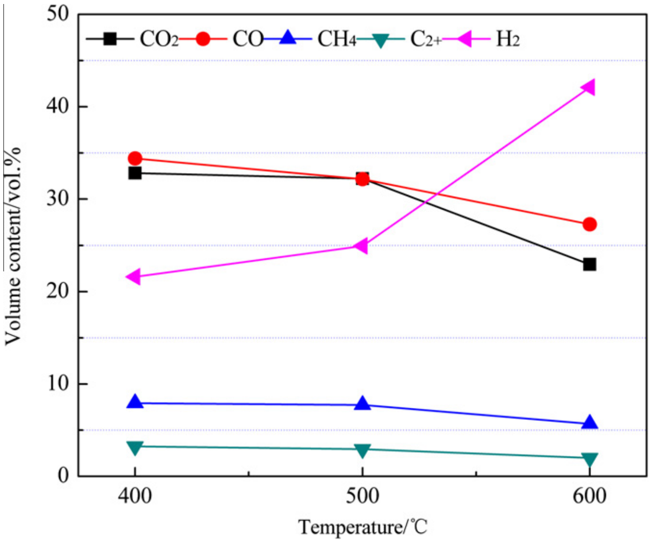

Fig. 5. Compositions of the gas products under different pyrolysis temperatures.

temperatures are consistent with the formation mechanisms of different gases and the effects of temperature on their formation (Yang et al., 2006b).

Based on the comprehensive analyzes of product distribution and composition, temperature is a very important factor in microwave pyrolysis. High temperature favors the increase in the yield of gas products and the ratio of combustible gas to total gas production, especially H_2 production (Dufour et al., 2009).

The calorific value of gas products can be calculated by the following formula (Dai et al., 2000) (LHV, kJ/m^3):

$$LHV = (30.0 \times CO + 25.7 \times H_2 + 85.4 \times CH_4 + 151.3 \times C_nH_m) \times 4.2 \qquad (3)$$

CO, H_2, CH_4, and C_mH_n are the volume percentage of CO, H_2, CH_4, and hydrocarbons (C_{2+}) in the total gas products, respectively.

The calorific value of the gas products was 11–12 MJ/Nm^3, indicating that the gases can be used as fuel or feed gas for the synthesis of chemicals.

3.4.3. Analysis of solid products under different pyrolysis temperatures

3.4.3.1. Analysis of the pore surface area and pore volume. The structural properties of coke obtained under different temperatures are shown in Table 2. Below 400 °C, there is no evidence for pyrolysis and only a few volatiles were released, consistent with the yield changes of coke and gases. As the temperature increased to 600 °C, the S_{BET} of coke increased from 0.89 m^2/g (400 °C) to 9.81 m^2/g (600 °C), but the average adsorption pore size d_{ave} dropped quickly from 282.16 nm (400 °C) to 46.64 nm (600 °C). This finding indicates that a large number of volatiles (e.g., CO_2, CO, etc.) were released with the increase in temperature, resulting in an increase in pore volume and specific surface area because the volatiles were produced faster and more homogeneously at a higher temperature. Consequently, a large number of small holes were opened because of the rapid release of volatiles. Thus, the number of pores of coke increased, the pore size decreased, and more uniform pore structure was obtained. The coke with the uniform pore structure and large surface area can be used as adsorbent by processing it into activated carbon (González et al., 2009).

Table 2
Specific surface area S_{BET}, average pore size d_{ave} and pore volume V_T under different temperatures of solid products.

Temperature (°C)	S_{BET} (m^2/g)	V_T (cm^3/g)	d_{ave} (Å)
400	0.89	0.006	282.16
500	3.33	0.010	118.59
600	9.81	0.012	46.64

Table 3
Elemental analyzes of solid products at different temperatures (wt.%).

Temperature (°C)	C	H	O[a]	N	S
400	52.18	2.79	37.30	1.06	0.77
500	53.01	2.49	36.26	0.94	1.40
600	53.67	2.34	35.49	0.92	1.68

[a] Subtraction; d-dry basis.

3.4.3.2. SEM. For an intuitive understanding of the pore structural characteristics of coke, the solid cokes obtained at different temperatures were analyzed using SEM. When the pyrolysis temperature was 400 °C, the surface pore structure of coke was relatively large, but the number of pores was small. However, at 600 °C, the surface pore structure was fine and dense, leading to a rapid increase in the specific surface area (Supplementary Fig. 4). The trend in the number of pores presented by the SEM images agreed with the results obtained by BET measurements.

3.4.3.3. Elemental analysis. As most volatiles were released during the pyrolysis process, the elemental composition of the solid residue underwent a drastic change. The main elements of solid cokes at different temperatures are tabulated in Table 3. C and O were the major elements, and a small amount of H, N, S, and other elements were also included. Below 400 °C, the contents of O and H decreased because of the removal of the OH bonds and condensation reactions (Yang et al., 2006a). More volatiles were also released with increasing temperatures, leading to a decrease in O and H contents. When the temperature exceeded 400 °C, the O content decreased with the increase in temperature, but the decreasing range was small. It fluctuated at a value of 36 wt.%, indicating that the cleavage of the oxygen-containing functional groups was concentrated in the low-temperature zone (Demirbas, 2000). The N content exhibited a slow downward trend with the increase in pyrolysis temperature; on the contrary, S showed a slow upwards trend. The reduction in N content may be due to the cleavage of nitrogen-containing functional groups and the release of nitrogen-containing gaseous products (Becidan et al., 2007).

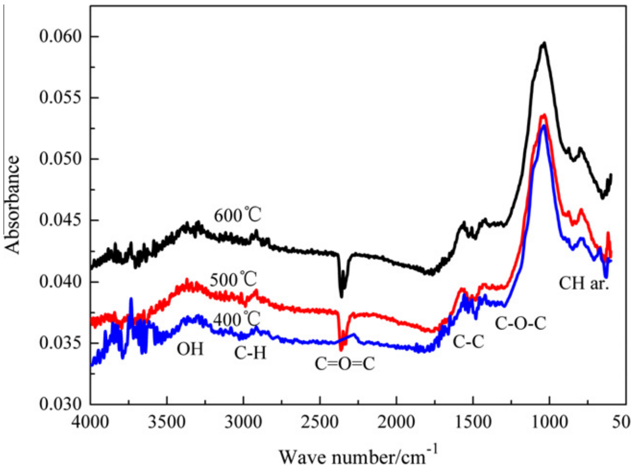

Fig. 6. IR spectrogram of solid coke under different pyrolysis temperatures.

3.4.3.4. Analysis of functional groups. Based on the IR spectrogram of solid coke in Fig. 6, the main functional groups of coke are OH (3400–3200 cm^{-1}, alcohol), C–H (2936–2916 cm^{-1}, olefin), $O{=}C{=}O$ (2350–2310 cm^{-1}), C–C (1475–1435 cm^{-1}, alkane, $R{-}CH_3$, $R'{-}CH_2{-}R'$ or aromatic ring), CO–(C) (1275 cm^{-1}), CO–(H)(1050 cm^{-1}) and C–H (865–810 cm^{-1}, C_{5+} olefin or aromatic ring).

The OH was removed, and its IR absorption band decreased rapidly when the temperature was only 400 °C. Moreover, the IR absorption band of C–H bond (olefins) decreased quickly with the temperature increase attributed to the rupture of weak alkyl C–H bonds, which favor the formation of gaseous hydrocarbons (Yang et al., 2006a). As a result, the yields of CH_4, C_2H_6, C_2H_4, etc. (400–500 °C) increased, whereas the content of element H in coke markedly decreased. The IR absorption band of $O{=}C{=}O$ (CO_2) remained at 400 °C, but with the increase in temperature, the IR absorption band of $O{=}C{=}O$ (CO_2) in coke rapidly decreased. The $C{=}O$ (1700 cm^{-1}) bonds within the samples were easily broken to form CO and CO_2, as there was no IR absorption band of $C{=}O$ bonds at the pyrolysis temperature of 400 °C.

4. Conclusions

From the results of this paper it was shown that the performance of the MWR that avoided condensation of volatiles which was favorable to product collection satisfied the requirements of precise experiments. The temperature was key parameter affecting the performance of microwave-induced pyrolysis. High temperature favorably increased the production of gas products. Moreover, the gas contained a higher concentration of syngas and lower concentrations of CO_2 and CH_4 with the increase in temperature. The potential of these gases as fuels and chemicals make them a valuable pyrolysis product. The higher amounts of H_2 can be attributed to the partial decomposition of CH_4 and the reformation of CH_4 by CO_2. It can be inferred that energy from biomass would not be a fantasy by the utilization of microwave pyrolysis. However, further experiments will be necessary, the results of which will be reported in due course.

Acknowledgements

This research project was financially supported by the National Natural Science Foundation of China (No. 50906047), Promotive research fund for excellent young and middle-aged scientists of Shandong Province (BS2011NJ011) and the Independent Innovation Foundation of Shandong University (IIFSDU No. 2010GN056).

Appendix A. Supplementary data

Supplementary data associated with this article can be found, in the online version, at doi:10.1016/j.biortech.2011.09.137.

References

Becidan, M., Skreiberg, Ø., Hustad, J.E., 2007. NOx and N_2O precursors (NH_3 and HCN) in pyrolysis of biomass residues. Energ. Fuel 21, 1173–1180.

Budarin, V.L., Clark, J.H., Lanigan, B.A., Shuttleworth, P., Breeden, S.W., Wilson, A.J., Macquarrie, D.J., Milkowski, K., Jones, J., Bridgeman, T., Ross, A., 2009. The preparation of high-grade bio-oils through the controlled, low temperature microwave activation of wheat straw. Bioresour. Technol. 100, 6064–6068.

Chen, M.Q., Wang, J., Zhang, M.X., Chen, M.G., Zhu, X.F., Min, F.F., Tan, Z.C., 2008. Catalytic effects of eight inorganic additives on pyrolysis of pine wood sawdust by microwave heating. J. Anal. Appl. Pyrolysis 82, 145–150.

Dai, X.W., Wu, C.Z., Li, H.B., Chen, Y., 2000. The fast pyrolysis of biomass in CFB reactor. Energ. Fuel 14, 552–557.

Demirbas, A., 2000. Mechanisms of liquefaction and pyrolysis reactions of biomass. Energ. Convers. Manage. 41, 633–646.

Di Blasi, C., Branca, C., Santoro, A., Perez, B.R.A., 2001. Weight loss dynamics of wood chips under fast radiative heating. J. Anal. Appl. Pyrolysis 57, 77–90.

Domínguez, A., Menéndez, J.A., Inguanzo, M., Bernad, P.L., Pis, J.J., 2003. Gas chromatographic–mass spectrometric study of the oil fractions produced by microwave-assisted pyrolysis of different sewage sludges. J. Chromatogr. A 1012, 193–206.

Domínguez, A., Menéndez, J.A., Inguanzo, M., Pís, J.J., 2006. Production of bio-fuels by high temperature pyrolysis of sewage sludge using conventional and microwave heating. Bioresour. Technol. 97, 1185–1193.

Domínguez, A., Fernández, Y., Fidalgo, B., Pis, J.J., Menéndez, J.A., 2007a. Biogas to syngas by microwave-assisted dry reforming in the presence of char. Energ. Fuel 21, 2066–2071.

Domínguez, A., Menéndez, J.A., Fernández, Y., Pis, J.J., Valente Nabais, J.M., Carrott, P.J.M., Ribeiro Carrott, M.M.L., 2007b. Conventional and microwave induced pyrolysis of coffee hulls for the production of a H_2 rich fuel gas. J. Anal. Appl. Pyrolysis 79, 128–135.

Dufour, A., Girods, P., Masson, E., Rogaume, Y., Zoulalian, A., 2009. Synthesis gas production by biomass pyrolysis: effect of reactor temperature on product distribution. Int. J. Hydrogen Energy 34, 1726–1734.

Encinar, J.M., Gonźalez, J.F., González, J., 2000. Fixed-bed pyrolysis of *Cynara cardunculus* L. product yields and compositions. Fuel Process. Technol. 68, 209–222.

Encinar, J.M., González, J.F., Martínez, G., Román, S., 2008. Catalytic pyrolysis of exhausted olive oil waste. J. Anal. Appl. Pyrolysis 85, 197–203.

González, J.F., Román, S., Encinar, J.M., Martánez, G., 2009. Pyrolysis of various biomass residues and char utilization for the production of activated carbons. J. Anal. Appl. Pyrolysis 85, 134–141.

Huang, H., Tang, L., 2008. Pyrolysis treatment of waste tire powder in a capacitively coupled RF plasma reactor. Energ. Convers. Manage. 50, 611–617.

Huang, Y.F., Kuan, W.H., Lo, S.L., Lin, C.F., 2008. Total recovery of resources and energy from rice straw using microwave-induced pyrolysis. Bioresour. Technol. 99, 8252–8258.

Huang, Y.F., Kuan, W.H., Lo, S.L., Lin, C.F., 2010. Hydrogen-rich fuel gas from rice straw via microwave-induced pyrolysis. Bioresour. Technol. 101, 1968–1973.

Lei, H.W., Ren, S.J., Julson, J., 2009. The effects of reaction temperature and time and particle size of corn stover on microwave pyrolysis. Energ. Fuel 23, 3254–3261.

Liu, X.T., Quan, X., Bo, L.L., Chen, S., Zhao, Y.Z., Chang, M., 2004. Temperature measurement of GAC and decomposition of PCP loaded on GAC and GAC-supported copper catalyst in microwave irradiation. Appl. Catal. A 264, 53–58.

Menéndez, J.A., Menéndez, E.M., Garcia, A., Parra, J.B., Pis, J.J., 1999. Thermal treatment of active carbons: a comparison between microwave and electrical heating. J. Microwave Power EE 34, 137–143.

Menéndez, J.A., Domínguez, A., Inguanzo, M., Pis, J.J., 2004. Microwave pyrolysis of sewage sludge: analysis of the gas fraction. J. Anal. Appl. Pyrolysis 71, 657–667.

Menéndez, J.A., Domínguez, A., Fernández, Y., Pis, J.J., 2007. Evidence of self-gasification during the microwave-induced pyrolysis of coffee hulls. Energ. Fuel 21, 373–378.

Miura, M., Kaga, H., Sakurai, A., Kakuchi, T., Takahashi, K., 2004. Rapid pyrolysis of wood block by microwave heating. J. Anal. Appl. Pyrolysis 71, 187–199.

Salema, A.A., Ani, F.N., 2011. Microwave induced pyrolysis of oil palm biomass. Bioresour. Technol. 102, 3388–3395.

Tu, W.K., Shie, J.L., Chang, C.Y., Chang, C.F., Lin, C.F., Yang, S.Y., Kuo, J.T., Shaw, D.G., You, Y.D., Lee, D.J., 2009. Products and bioenergy from the pyrolysis of rice straw via radio frequency plasma and its kinetics. Bioresour. Technol. 100, 2052–2061.

Wan, Y., Chen, P., Zhang, B., Yang, C., Liu, Y., Lin, X., Ruan, R., 2009. Microwave-assisted pyrolysis of biomass: catalyst to improve product selectivity. J. Anal. Appl. Pyrolysis 86, 161–167.

Wang, X.H., Chen, H.P., Ding, X.J., Yang, H.P., Zhang, S.H., Shen, Y.Q., 2009. Properties of gas and char from microwave pyrolysis of pine sawdust. Bioresources 4, 946–959.

Yagmur, E., Ozmaka, M., Aktas, Z., 2008. A novel method for production of activated carbon from waste tea by chemical activation with microwave energy. Fuel 87, 3278–3285.

Yang, H.P., Yan, R., Chen, H.P., Lee, D.H., Liang, D.T., Zheng, C.G., 2006a. Mechanism of palm oil waste pyrolysis in a packed bed. Energ. Fuel 20, 1321–1328.

Yang, H.P., Yan, R., Chen, H.P., Lee, D.H., Liang, D.T., Zheng, C.G., 2006b. Pyrolysis of palm oil wastes for enhanced production of hydrogen rich gases. Fuel Process. Technol. 87, 935–942.

Yu, F., Ruan, R., Deng, S.B., Chen, P., Lin, X.Y., 2006. Microwave pyrolysis of biomass. An ASABE Meeting Presentation Paper, No. 066051.

Zhao, X.Q., Song, Z.L., Liu, H.Z., Li, Z.Q., Li, L.Z., Ma, C.Y., 2010. Microwave pyrolysis of corn stalk bale: a promising method for direct utilization of large-sized biomass and syngas production. J. Anal. Appl. Pyrolysis 89, 87–94.

Zuo, W., Tian, Y., Ren, N.Q., 2011. The important role of microwave receptors in bio-fuel production by microwave-induced pyrolysis of sewage sludge. Waste Manage. 31, 1321–1326.